Reforming of C7 hydrocarbons on a sulfided commercial Pt/Al2O3 catalyst

Reforming of C_7 Hydrocarbons on a Sulfided Commercial Pt/Al_2O_3 Catalyst

P. A. Van Trimpont, G. B. Marin, and G. F. Froment*
Laboratorium voor Petrochemische Techniek, Rijksuniversiteit Gent, B-9000 Gent, Belgium

The kinetics of the reforming of C_7 hydrocarbons were studied in a tubular reactor on a sulfided commercial Pt/Al_2O_3 catalyst under both deactivating and nondeactivating conditions. The temperature was varied from 582 to 763 K, the total pressure from 3 to 21 bar, and the hydrogen partial pressure from 2 to 20 bar. The bifunctional reforming reactions were best described by Hougen–Watson rate equations corresponding to a single-site surface reaction on the acid function as the rate-determining step. Electrobalance experiments showed that the isomerization rate, the dehydrogenation rate, and the coking rate exponentially decrease with coke content. The coking rate equations were derived from the regression of the ascending coke content profiles obtained in the tubular reactor after experiments under deactivating conditions. Coke deposition mainly originates from highly unsaturated C_7 naphthenes, such as cyclopentadienes and methylcyclohexadienes.

Introduction

Catalytic reforming is a process enhancing the octane number of naphtha so as to improve its performance as motor gasoline. Legal restrictions on the addition of lead containing antiknock components can be compensated for by reforming the naphtha under more severe conditions, but these also cause an increase of the rate of coke deposition. A detailed kinetic model for the reforming of naphtha is required for the optimization of existing plants or the design of new ones. Previous work from this laboratory dealt with the reforming of C_5 and C_6 naphtha components (Hosten and Froment, 1971; Lambrecht and Froment, 1972; De Pauw and Froment, 1975; Marin and Froment, 1982) and with the dehydrogenation of methylcyclohexane into toluene on a sulfided commercial Pt/Al_2O_3 catalyst under nondeactivating conditions (Van Trimpont et al., 1986). The present work extends the kinetic study to the complete C_7 fraction under both deactivating and nondeactivating conditions.

Experimental Section

Equipment and Procedure. The experimental equipment has been described in detail before (De Pauw and Froment, 1975; Marin and Froment, 1982).

The tubular stainless steel reactor consisted of a mixing section of 260-mm length filled with inert packing followed by seven to nine catalyst layers separated by inert packing. To ensure isothermal operation, the catalyst layers were diluted up to a volume ratio of five. The pretreatment and presulfidation of the catalyst have been reported earlier (Van Trimpont et al., 1986) and were followed by feeding 0.5 mol h^{-1} of *n*-heptane containing 128 wt ppm sulfur as thiophene at 693 K, 20.5 bar, and a molar H_2 to hydrocarbon ratio of 40 during 20 h. The experimental program under nondeactivating conditions and with heptane as feed was carried out on a single catalyst batch of 108.7 g. A standard test on the reproducibility of the catalyst activity and selectivities was periodically performed at the conditions under which the stabilization had been performed. Each experiment under deactivating conditions was performed on a new batch of catalyst.

The catalyst pretreatment in the electrobalance setup consisted of a calcination at 773 K by 30 nL h^{-1} of air for 2 h. After the catalyst mass (typically 0.5 g) was cooled to room temperature, reduction was started. The temperature was raised at a rate of 10 K min^{-1} until it reached 773 K under a H_2 stream of 30 nL h^{-1}. The temperature was maintained at 773 K for 3 h. Presulfidation was carried out until H_2S breakthrough at 673 K with a gas mixture of 99 vol % H_2 and 1 vol % H_2S. The weakly held sulfur was stripped off at 773 K with hydrogen.

Conditions. The commercial reforming catalyst contained 0.593 wt % Pt and 0.67 wt % Cl on a γ-Al_2O_3 support. Its BET surface area amounted to 192 m^2 g^{-1}, and the fraction of exposed platinum atoms to 0.48. The absence of external transport limitations was checked both theoretically and experimentally. Internal diffusion limitations were avoided by using catalyst particles with diameters between 0.4 and 1.0 mm.

The hydrocarbon feed was either *n*-heptane with a purity higher than 99% or technical heptane containing 39.6% isoheptanes, 33.8% *n*-heptane, 9.9% cyclopentanes, 15.2% methylcyclohexane, 0.3% toluene, and 1.2 mol % C_5 and C_6 hydrocarbons. The sulfur content of both feedstocks was lower than 0.5 ppm. The feed was dried on a Ca–A zeolite. The hydrogen (purity of 99.999%) was further deoxygenated over a Pt catalyst at 573 K and dried over a Ca–A zeolite at room temperature.

Thiophene was added to the hydrocarbon feed in order to maintain a constant molar H_2S to H_2 ratio of 10^{-5} during the experiments. It was shown previously (Menon et al., 1982; Van Trimpont et al., 1985) that such a ratio corresponds to a molar sulfur to surface Pt ratio close to one and allows a suppression of the hydrogenolysis activity without a too pronounced attenuation of the dehydrogenation activity.

Deactivation due to coking could be neglected at hydrogen partial pressures higher than 10 bar. A total of 11 conversions vs $W/F_{HC}°$ curves were determined at total pressures ranging from 10.5 to 21 bar, hydrocarbon inlet partial pressures from 0.15 to 0.5 bar, and temperatures from 693 to 723 K. The $W/F_{HC}°$ ratio varied between 8.5 and 561 (kg of catalyst h)/kmol.

A separate set of experiments was performed to study the dehydrogenation of methylcyclohexane into toluene. The conditions and the kinetic analysis of these experiments are reported elsewhere (Van Trimpont et al., 1986).

Four runs under deactivating conditions, given in Table I, were carried out in the tubular reactor. For each of them a fresh catalyst batch was loaded. After the standard pretreatment, the deactivation experiment lasted 9–10 h. The isomerization of *n*-heptane into methylhexanes in the presence of coking was also studied in a differentially operated electrobalance at 763 K, 3 bar, and a molar H_2 to hydrocarbon ratio of 2. No sulfur was added to the feed. A similar experiment was performed with methylcyclohexane.

0888-5885/88/2627-0051$01.50/0

Table I. Experiments Performed under Deactivating Conditions in the Tubular Reactor

	expt no.			
	1	2	3	4
temp, K	763	743	723	763
p_{nP_7}, bar	1	1	1	1
p_H, bar	2	2	2	3
$F_{HC}°$, mol/h	2.84	2.58	2.56	2.08
sulfur content, wt ppm	6.4	6.4	6.4	9.6
run length, h	9.83	9.57	10.07	8.88
catalyst mass, g	64.8	90.4	89.9	78.9

Table II. Selectivities for Isoheptanes[a]

	conversion, %		
component	1.7	2.6	27.8
2,2-dimethylpentane, %			1.1
2,4-dimethylpentane, %			1.4
3,3-dimethylpentane, %			2.1
2,3-dimethylpentane, %		1.1	6.5
2-methylhexane, %	25.6	27.9	30.3
3-methylhexane, %	55.3	55.9	46.4
3-ethylpentane, %	1.2	1.1	2.9

[a] At 693 K, 20.5 bar, and molar H_2 to *n*-heptane inlet ratio of 40.

Table III. Distribution of Ring Closure and Cracked Products of *n*-Heptane[a]

ring-closure products	mol, %	cracked products	mol, %
1,1-dimethylcyclopentane		methane	
1,*cis*-3-dimethylcyclopentane		ethane	18.7
1,*trans*-3-dimethylcyclopentane	33.8	propane	37.5
1,*trans*-2-dimethylcyclopentane	16.2	isobutane	
1,*cis*-2-dimethylcyclopentane	27.9	*n*-butane	31.3
ethylcyclopentane	22.1	isopentane	
methylcyclohexane		*n*-pentane	12.5
		isohexanes	
		n-hexane	

[a] At $W/F_{HC}°$ = 0 (kg of catalyst h)/mol, 693 K, 20.5 bar and a molar H_2 to *n*-heptane ratio of 40.

Kinetic Analysis

Construction of the Reaction Network. Tables II, III, and IV allow one to obtain an insight into the reaction paths of reforming. Table II shows that the primary isomerization products of *n*-heptane are methylhexanes. Ethylpentane and multibranched paraffins are only observed at higher conversions. It follows from the first part of Table III that ring closure proceeds through the formation of a five-ring structure. Direct six-ring closure is not observed. A distribution of cracked products of *n*-heptane is shown in the second part of Table III. The distribution is consistent with hydrocracking, i.e., bifunctional cracking. Similar observations concerning the isomerization, the ring closure, and the cracking of C_6 hydrocarbons were made by Marin and Froment (1982) and resulted in a detailed reaction network for the reforming of C_6 hydrocarbons. The derived reaction network for the C_6 fraction linked 8 components, including the

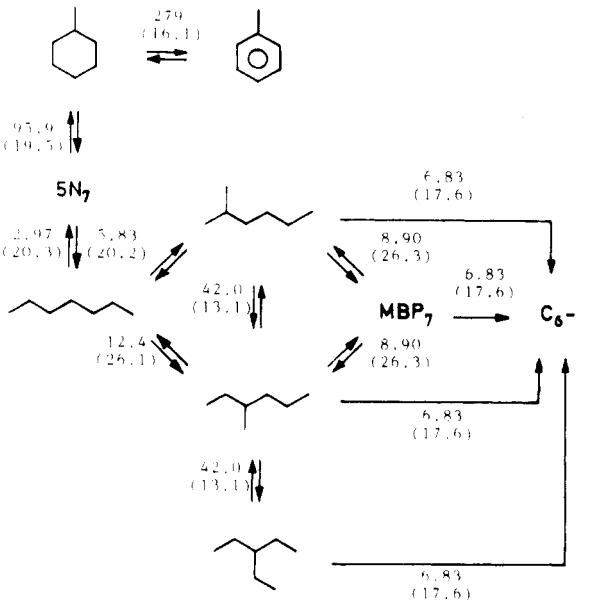

Figure 1. Reaction network and first-order rate coefficients (10^{-3} kmol/(kg of catalyst h bar)) for the catalytic reforming of C_7 hydrocarbons at 693 K, 10.5 bar, and a molar H_2/*n*-heptane inlet ratio of 20. *t* values in parentheses.

lumped cracked products, by 12 reaction paths. The corresponding detailed reaction network for the reforming of C_7 hydrocarbons consists of 14 hydrocarbons linked by at least 26 reaction paths and has a completely analogous structure.

Figure 1 shows a reaction network for the reforming of C_7 hydrocarbons with lumped multibranched isoheptanes and lumped cyclopentanes. The lumping of the multibranched isoheptanes can be justified by the high rates of isomerizations which do not involve a change in degree of branching (Kuo and Wei, 1969; Marin and Froment, 1982). This is illustrated in Figure 1 by the difference between the first-order rate coefficients for the isomerizations among single-branched isoheptanes and for the isomerizations between *n*-heptane and single-branched isoheptanes. The lumping of the cyclopentanes is justified by the observations reported in Table IV: the disubstituted cyclopentanes are present in proportions close to thermodynamic equilibrium, indicating much higher reaction rates among them than between them and the other components. Although ethylcyclopentane is not in equilibrium with the disubstituted cyclopentanes, its concentration is sufficiently low to allow lumping with the latter. It also follows from Table IV that methylcyclohexane is not in equilibrium with the cyclopentanes, so that it cannot be included in the lump. The above considerations lead to a reduced reaction network for the reforming of C_7 hydrocarbons, shown in Figure 2, which will be used for the further kinetic analysis of the experimental data.

Table V compares some of the first-order rate coefficients shown in Figure 1 with the corresponding first-order

Table IV. Molar Ratios of C_7 Naphthenes[a]

mole fraction ratios	exptl value				value at thermodynamic equilibrium
1,*cis*-2-DMCP/1,*trans*-2-DMCP	0.19	0.24	0.21	0.19	0.28
1,*cis*-3-DMCP/1,*trans*-3-DMCP	1.62	1.48	1.40	1.40	1.45
1,2-DMCP/1,3-DMCP	0.78	0.94	0.99	0.97	0.87
ECP/DMCP	0.02	0.02	0.02	0.03	0.26
$5N_7/6N_7$	9.1	12.4	13.8	9.3	0.26
n-heptane convn, %	27.7	45.5	60.4	76.3	

[a] At 693 K, 3 bar, and a molar H_2 to hydrocarbon inlet ratio of 2.

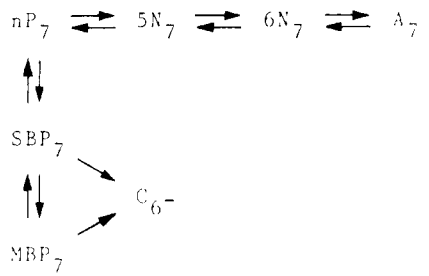

Figure 2. Lumped reaction network for the reforming of C_7 hydrocarbons.

Table V. Relative First-Order Rate Coefficients for Reactions of Hexanes[a] and Heptanes[b]

reaction	$k/k_{nP_6\rightarrow MCP}$	reaction	$k/k_{nP_6\rightarrow MCP}$
$nP_6 \rightleftarrows 2MP$	25	$nP_7 \rightleftarrows 2MH$	36
$nP_6 \rightleftarrows 3MP$	22	$nP_7 \rightleftarrows 3MH$	77
$2MP \rightleftarrows 3MP$	78	$2MH \rightleftarrows 3MH$	263
$2MP \rightleftarrows 2,3\text{-DMB}$	18	$2MH \rightleftarrows MBP_7$	56
$2MP + H_2 \rightarrow 2C_5^-$	7.4	$2MH + H_2 \rightarrow 2C_6^-$	43
$3MP + H_2 \rightarrow 2C_5^-$	8.6	$3MH + H_2 \rightarrow 2C_6^-$	43
$2,2\text{-DMB} + H_2 \rightarrow 2C_5^-$	19	$MBP_7 + H_2 \rightarrow 2C_6^-$	43
		$nP_7 \rightleftarrows 5N_7 + H_2$	19
$nP_6 \rightleftarrows MCP + H_2$	1.0	$5N_7 \rightleftarrows MCH$	600
$MCP \rightleftarrows Bz + 3H_2$	42		

[a] At 693 K, 10 bar, molar hydrogen to hydrocarbon ratio of 10, and molar H_2S to H_2 ratio of 10^{-4}. [b] At 693 K, 10.5 bar, molar hydrogen to hydrocarbon ratio of 20, and molar H_2S to H_2 ratio of 10^{-5}.

rate coefficients for the C_6 fraction reported by Marin and Froment (1982) but obtained at a H_2S to H_2 ratio 10 times higher than in the present work. At 693 K, the rate coefficients for isomerization and hydrocracking of the C_7 fraction are 3–5 times higher than those obtained for the C_6 fraction. The relative values of the isomerization rate coefficients within a given fraction depend only weakly on the carbon number. The ratio of the rate of cracking to that of isomerization is higher for the C_7 fraction. Cracking of *n*-hexane and *n*-heptane can be neglected in comparison to the cracking of the isoparaffins. No distinction can be made between the hydrocracking rates of the single-branched and the multibranched isoheptanes. Ring closure is the slowest reaction for both fractions, but the ring closure of *n*-heptane is much faster than that of *n*-hexane. Analogous observations hold for ring expansion. The observed differences between the C_6 fraction and the C_7 fraction can mainly be attributed to differences between the stability of the corresponding carbenium ion intermediates as well as between the number of available reaction paths. The higher rate for ring closure of *n*-heptane in particular is caused by the higher stability of the intermediate disubstituted protonated triangular structure proposed by Callender et al. (1973) and Brandenberger et al. (1976). The higher rate of ring expansion of the C_7 five-ring naphthenes is explained in a similar way.

Parameter Estimation and Model Discrimination Procedure. The data analysis was performed as outlined by Froment and Hosten (1981) and according to the integral method. The response vector consisted of the conversions into six independent components of the network shown in Figure 2: the single-branched and multibranched isoheptanes, the cracked products, the cyclopentanes, methylcyclohexane, and toluene. *n*-Heptane and hydrogen were obtained from the C and H mass balances. The calculated conversions are obtained from the rates, r_i, by integrating the corresponding continuity equations. When the quasi-steady-state approximation can be applied to the gas-phase components, i.e., when the time scale of the deactivation is much larger than the time scale of the reforming reactions, the continuity equations reduce to ordinary differential equations (Marin and Froment, 1982)

$$\mathrm{d}\mathbf{x}/\mathrm{d}(W/F_{HC}^\circ) = \mathbf{R} \qquad \text{at constant } t \tag{1}$$

$$\mathrm{d}C_C/\mathrm{d}t = R_C \qquad \text{at constant } W/F_{HC}^\circ \tag{2}$$

where

$$x_j = (F_j - F_j^\circ)/F_{HC}^\circ \qquad R_j = \sum_k s_{ij} r_i \qquad R_C = \sum_k r_{Ck}$$

and with initial and boundary conditions

$$\mathbf{x} = 0 \quad \text{at} \quad W/F_{HC}^\circ = 0, \quad t \geq 0$$

$$C_C = 0 \quad \text{at} \quad t = 0, \quad 0 \leq W/F_{HC}^\circ \leq W_t/F_{HC}^\circ$$

Equation 2, the continuity equation for the coke, is obviously only considered under deactivating conditions.

Maximum-likelihood parameter estimates were obtained by minimizing the weighted sum of squares and cross-products of the residuals between the observed and calculated conversions.

Kinetics of Reforming Reactions in the Absence of Coking. Hougen–Watson rate equations were derived for each of the reactions shown in the lumped reaction network of Figure 2 on the basis of a priori possible reaction mechanisms. The discrimination procedure for the rate equation for the metal-catalyzed dehydrogenation of methylcyclohexane into toluene is described elsewhere (Van Trimpont et al., 1986), and the selected rate equation is shown in Table VI. The remaining reactions are bifunctional; i.e., they involve both the metal and the acid function of the catalyst (Heinemann et al., 1954). The elementary steps involving the surface of the acid alumina support are rate-determining (Hosten and Froment, 1971; De Pauw and Froment, 1975; Marin and Froment, 1982). Both single- and dual-site mechanisms were considered for the surface reactions on the support. Hydrocracking was considered to occur either with or without the involvement of molecular hydrogen according to a Rideal mechanism.

A statistical discrimination between the same eight rival combinations of rate equations as those already considered for the bifunctional reforming reactions of C_6 hydrocarbons by Marin and Froment (1982) was performed. Nine hundred ninety-six experimental conversion obtained with

Table VI. Reaction Rate Equations, Parameter Estimates, and *t* Values[a] Obtained by Analyzing the Experimental Conversions under Nondeactivating Conditions

	A_0[b]	E, kJ/mol
isomerization $r^\circ = A_0 e^{-E/RT}(p_A - p_B/K_{A\text{-}B})/(p_H\Gamma)$	1.83×10^6 (7.9)	87.75 (15)
hydrocracking $r^\circ = A_0 e^{-E/RT} p_A/\Gamma$	1.43×10^{17}[c] (7.5)	256.4 (29)
ring closure $r^\circ = A_0 e^{-E/RT}(p_A - p_B p_H/K_{A\text{-}B})/(p_H\Gamma)$	2.48×10^{17} (6.8)	256.4 (29)
ring expansion $r^\circ = A_0 e^{-E/RT}(p_A - p_B/K_{A\text{-}B})/(p_H\Gamma)$	9.08×10^{17} (5.5)	256.4 (29)
dehydrogenation of methylcyclohexane $r^\circ = A_0 e^{-E/RT}(p_A - p_B p_H^3/K_{A\text{-}B})/(p_H\theta)^2$	1.47×10^4[d] (23)	42.60 (24)

Adsorption Term for the Acid Function

$\Gamma = (p_H + K_{C_6^-}p_{C_6^-} + K_{P_7}p_{P_7} + K_{N_7}p_{N_7} + K_{Tol}p_{Tol}p_H)/p_H$
$K_{C_6^-} = 107$ (2.9); $K_{P_7} = 21.9$ (5.2); $K_{N_7} = 659$ (6.1);
$K_{Tol} = 70.3$ bar^{-1} (3.7)

Adsorption Term for the Metal Function

$\theta = 1 + K_{MCH}p_{MCH} + Ae^{-\Delta H^\circ/RT}(p_{MCH}/p_H^2)$
$K_{MCH} = 0.27$ bar^{-1}; $A = 8.34 \times 10^9$ bar; $\Delta H^\circ = 96.93$ kJ/mol

[a] In parentheses. [b] Units of kmol/(kg of catalyst h) unless noted otherwise. [c] Units of kmol/(kg of catalyst h bar). [d] Units of (kmol bar)/(kg of catalyst h).

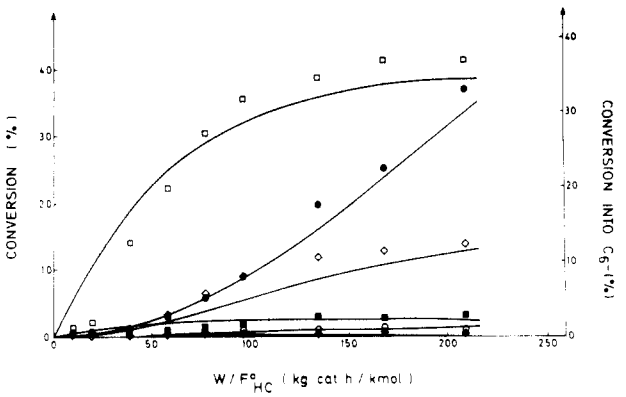

Figure 3. Conversion vs W/F_{HC}° curves at 693 K, 20.5 bar, and a molar H_2 to hydrocarbon inlet ratio of 40 with *n*-heptane as feed. Full lines, calculated with the rate equations of Table VI. Points, experimental: (□) SBP_7; (●) C_6–; (◇) MBP_7; (■) Tol; (○) $5N_7$; (◆) MCH.

n-heptane, technical heptane, and methylcyclohexane feed under conditions where coke deposition could be neglected were regressed. The estimates for the parameters in the adsorption term corresponding to the metal function were obtained from the regression of the data with methylcyclohexane feed alone and by taking into account the temperature dependence of the adsorption coefficient of toluene.

The most detailed expression for the adsorption term corresponding to the acid function accounts for the competitive adsorption between heptenes, unsaturated cracked products, naphthenes, and toluene. The estimates of the apparent adsorption coefficients of *n*-heptane and the single-branched and multibranched heptanes were not significantly different from one another at the 95% probability level. Since also the difference between the estimates of the apparent adsorption coefficients of the cyclopentanes and methylcyclohexane was not significant, a single apparent adsorption coefficient was introduced for the heptanes and the naphthenes. For analogous reasons a single apparent activation energy was introduced to take into account the temperature dependence of the hydrocracking, the five-ring closure, and the ring expansion. Also, no distinction was retained between the preexponential factors and the apparent activation energies for the isomerizations. Considering the temperature dependence of the apparent adsorption coefficients did not result in an increase of the significance of the global regression. The best global regression was obtained with the rate equations shown in Table VI. The rate equations for the bifunctional reforming reactions correspond to the single-site surface reaction on the acid function as the rate-determining step. A comparison between experimental and calculated conversion vs W/F_{HC}° curves is shown in Figure 3 for typical conditions under which deactivation can be neglected.

The set of rate equations selected by Marin and Froment (1982) for the reforming of C_6 hydrocarbons is identical with the rate equations for the bifunctional reactions reported in Table VI, except for the exponent of the denominator for which a value of two was obtained, reflecting a dual-site rate-determining step on the acid function. The experimental pressures covered by Marin and Froment (1982) varied between 1.6 and 16 bar, i.e., over a factor of 10 as compared to a factor of 2 in the present work. Deactivation due to coking required extrapolation to zero process time of the C_6 reforming data obtained at low pressures. The inclusion of the experiments at low pressures was necessary to obtain an accurate determination of the apparent adsorption coefficients. The rate equations for the reforming of C_6 hydrocarbons corresponding to a single-site rate-determining step on the acid function led to a global regression with an F value higher than the one corresponding to a dual-site rate-determining step. Yet, they were not retained because of the lower significance of the apparent adsorption coefficient for the hexanes (Marin, 1980). The corresponding estimate for the apparent adsorption coefficient amounted to 89, with a t value of 5, which reasonably agrees with the estimate of 107 for the apparent adsorption coefficient of the C_6 hydrocarbons listed in Table VI. The estimates for the activation energies did not depend on the exponent of the denominator of the rate equations. The activation energy for isomerization of C_6 hydrocarbons is lower than the corresponding activation energy listed in Table VI. The activation energies for hydrocracking and for ring expansion are higher for C_6 hydrocarbons, whereas that for ring closure with C_6 hydrocarbons is close to that for ring closure with C_7 hydrocarbons.

Kinetics of Reforming Reactions in the Presence of Coking

Selection of the Deactivation Functions. Coke deposition causes a deactivation of the catalyst which can be described by introducing a deactivation function, ϕ_i, that multiplies the reaction rates at zero coke content:

$$r_i = r_i^{\circ}\phi_i \qquad 0 \le \phi_i \le 1 \tag{3}$$

The same approach can be taken to describe the decrease of the coking rates, r_{Ck}:

$$r_{Ck} = r_{Ck}^{\circ}\phi_{Ck} \qquad 0 \le \phi_{Ck} \le 1 \tag{4}$$

Equations 3 and 4 assume that the rate equations are separable. The separability of the reforming rate equations was found to be valid for the C_6 fraction by Marin and Froment (1982). The deactivation functions were related to the cause of the deactivation, i.e., the coke content of the catalyst, and not to process time, as is frequently done (Froment, 1977). No distinction was made between coke deposited on the acid function and coke deposited on the metal function. Several empirical expressions for the deactivation functions were statistically tested by regressing rate data on the isomerization of *n*-heptane into single-branched isoheptanes and the corresponding coke content data obtained in the electrobalance setup. The deactivation function for the isomerization was determined by measuring simultaneously the coke content and the composition of the exit gases as a function of time. The conversions were referred to the one first measured. Elimination of time led to the experimental points shown in Figure 4. An exponentially decreasing function, $\phi = e^{-\alpha C_C}$, led to the best global regression for both the isomerization and the coking data, as was found before by De Pauw and Froment (1975) and Marin and Froment (1982). The corresponding calculated deactivation function for the isomerization of *n*-heptane is also shown in Figure 4. Similar observations were made for the dehydrogenation of methylcyclohexane into toluene.

Estimation of the Deactivation Constants. With an exponentially decreasing deactivation function, integration of the continuity equation for coke (eq 2) yields

$$C_C = (1/\alpha_C) \ln (1 + \alpha_C R_C^{\circ} t) \tag{5}$$

where R_C° is the rate of coke production corresponding to the feed composition. Equation 5 assumes a single deactivation function for the coking reactions:

$$\phi_C = e^{-\alpha_C C_C} \tag{6}$$

An estimate of 24.18 kg of catalyst/kg of coke with an

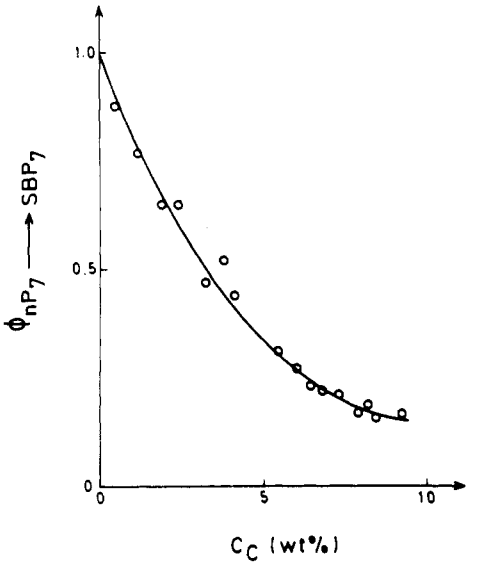

Figure 4. Deactivation function, $\phi_{nP_7 \rightarrow SBP_7} = e^{-\alpha C_C}$, vs coke content obtained on the electrobalance setup at 763 K, 3 bar, and a molar H_2 to *n*-heptane ratio of 2: (points) experimental; (full lines) calculated.

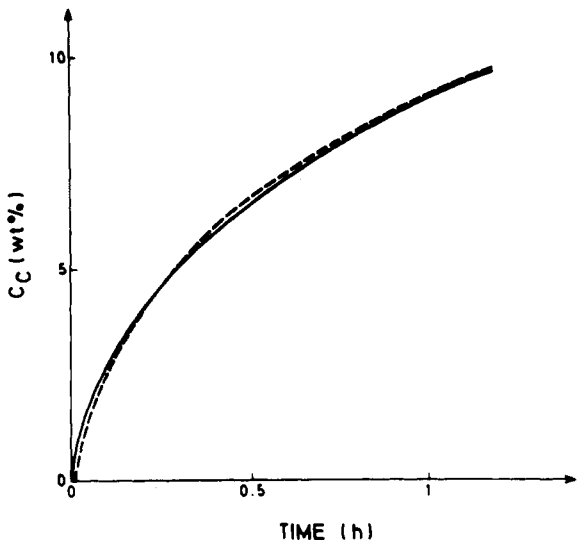

Figure 5. Coke content vs time obtained in the electrobalance setup at 763 K, 3 bar, and a molar H_2 to *n*-heptane ratio of 2: (dashed line) experimental; (full line) calculated from eq 5.

individual t value of 73.5 was obtained for the deactivation constant, α_C. A comparison between experimental and calculated results is shown in Figure 5.

Since the rate-determining steps of the bifunctional reforming reactions all occur on the acid function and involve the same number of sites, a single exponentially decreasing deactivation function was introduced to describe the decrease of the corresponding reaction rates:

$$\phi_A = e^{-\alpha_A C_C} \tag{7}$$

The deactivation constant, α_A, was determined together with the deactivation constant for the metal-catalyzed dehydrogenation of methylcyclohexane into toluene, α_M, by regression of 3528 experimental conversions observed in the tubular ractor under the deactivation conditions listed in Table I. The integration of the continuity equations for the gas-phase components, eq 1, requires the knowledge of the catalyst coke content at intermediate process times. The experiments in the tubular reactor provided only coke contents at the end of an experimental run, however. Therefore, intermediate coke contents were

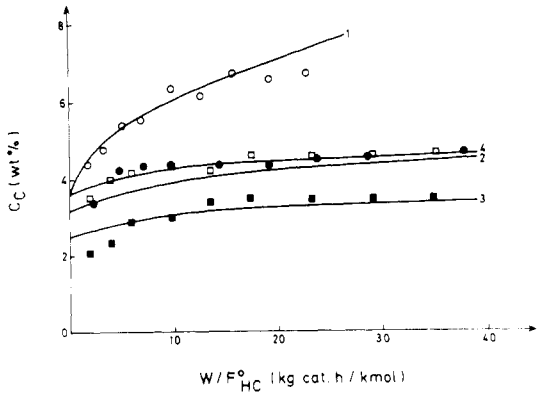

Figure 6. Calculated and experimental final coke content profiles: (points) experimental, numbers corresponding to Table I; (full lines) coke contents calculated by integration of eq 2.

obtained from eq 5 with $R_C^\circ(z_i,t_j)$ calculated from the observed final coke content:

$$C_C(z_i,t_j) = \frac{1}{\alpha_C} \ln\left(1 + \frac{e^{\alpha_C C_C(z_i,t_f)} - 1}{t_f} t_j\right) \tag{8}$$

The absence of observed intermediate coke contents did not allow the estimation of the deactivation constant corresponding to the coking rate, α_C, from the data obtained in the tubular reactor setup. Only when α_C is set equal to either α_A or α_M can an estimate for α_C be obtained (Marin and Froment, 1982). In the present work a better global regression of the data collected in the tubular reactor setup was obtained by using in eq 8 the value of α_C estimated from the electrobalance experiments. This led to the following estimates and t values for the two deactivation constants corresponding to the reforming reactions

$$\alpha_A = 14.95, \quad t_{\alpha_A} = 20; \qquad \alpha_M = 16.79, \quad t_{\alpha_M} = 28$$

in kilograms of catalyst per kilogram of coke.

Coking Kinetics. Figure 6 shows the observed coke content profiles at the end of each of the four deactivation runs performed in the tubular reactor. The ascending coke content profiles can be explained in terms of coking from reaction products (Froment and Bischoff, 1961, 1962). The coke content is not zero at the inlet of the bed, however. This implies that coke deposition also originates from the feed, *n*-heptane, or from components in equilibrium with *n*-heptane, such as *n*-heptenes or *n*-heptadienes. The coke formation increases with increasing temperatures and decreasing hydrogen partial pressures. The trends shown in Figure 6 agree with those observed for C_6 hydrocarbons (Marin and Froment, 1982).

Rate equations for the coke deposition were derived by regression of the observed final coke contents. The parameter estimation and model discrimination procedure was performed as outlined by Marin and Froment (1982) and is schematically represented in Figure 7. In the present case, however, the partial pressures of the hydrocarbons and hydrogen, $p(z_i,t_j)$, used for the calculation of the final coke contents, $C_C(z_i,t_f)$, were not the partial pressures obtained by the integration of the continuity equations for the gas-phase components, eq 1, but those from the experimentally observed partial pressures. A total of 24 reaction paths for coke formation was considered. Homogeneous rate equations resulted into a better global regression than the corresponding rate equations with an adsorption term. Three significant contributions to coke formation were selected by the model discrimination procedure. They are shown schematically in Table VII together with the corresponding parameter estimates. The

Table VII. Reaction Schemes, Rate Equations, and Parameter Estimates for Coke Formation[a]

C_7 hydrocarbons	C_6 hydrocarbons
Coking Schemes	
$Tol + 5N^{2=}_7 \rightarrow C_{P_1}$	$2MCP^{2=} \rightarrow C_{P_4}$
$Tol + MCH^{2=} \rightarrow C_{P_2}$	$Bz + MP^{2=} \rightarrow C_{P_5}$
$n\text{-}P^{=}_7 \rightarrow C_{P_3}$	
Rate Equations	
$R_C^\circ = k_{C_1}\frac{p_{Tol}p_{5N_7}}{p_{H^2}} + k_{C_2}\frac{p_{Tol}p_{MCH}}{p_{H^2}} + k_{C_3}\frac{p_{nP_7}}{p_H}$	
$R_C^\circ = k_{C_4}\left(\frac{p_{5N_6}}{p_{H^2}}\right)^5 + k_{C_5}\frac{p_{SBP_6}p_{Bz}}{p_{H^2}}$	

	scheme				
	1	2	3	4	5
	Parameters Estimates[a]				
$A_{0,C}$[b]	7.51×10^5 (6.2)	1.00×10^6 (3.3)	1.01×10^2 (5.6)	3.18×10^{16} (24)	3.77×10^2 (10)
E, kJ/mol	58.64 (6.8)	58.64 (6.8)	58.64 (6.8)	205.7 (18)	58.94 (1.7)

[a] Approximate individual t values are given in parentheses. [b] Units of kg of coke/(kg of catalyst h) for schemes 1–3 and 5; units of (kg of coke bar^2)/(kg of catalyst h) for scheme 4.

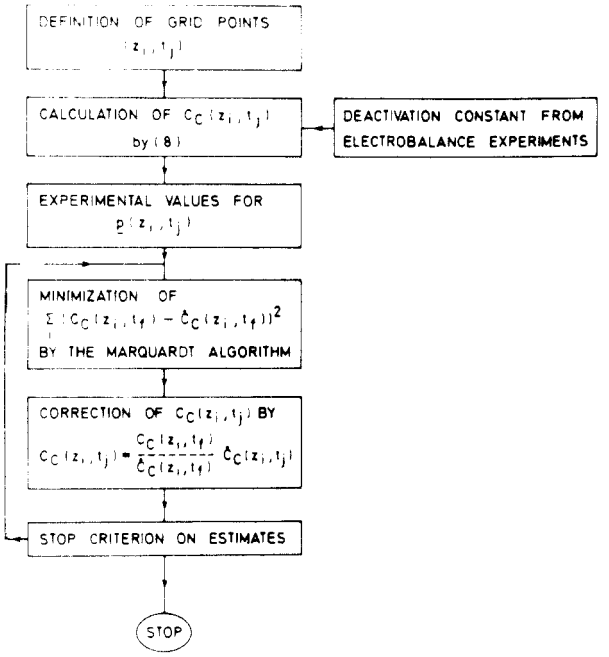

Figure 7. Parameter estimation procedure for the coking rate equations.

calculated coke content profiles are shown in Figure 6. The two contributions corresponding to intercondensation reactions between toluene and C_7 cyclopentadienes and between toluene and methylcyclohexadiene are the most important ones. The third contribution to coke formation originates from *n*-heptenes and accounts for the parallel coke deposition observed with *n*-heptane as feedstock, i.e., for the coke contents measured at the reactor inlet.

Table VII also allows a comparison between the coke deposition originating from a C_7 feedstock and that originating from a C_6 feedstock (Marin and Froment, 1982). For both fractions strongly dehydrogenated naphthenes are the most important gas-phase intermediates leading to cokes. This is in accordance with the observations of other authors (Bakulin et al., 1978; Parera et al., 1984; Barbier et al., 1984a). The initial coking rates corresponding to the C_7 fraction are 10 times higher than those corresponding to the C_6 fraction under the conditions used for the accelerated deactivation runs in the present work. The difference is even more pronounced under typical industrial conditions. It should be kept in mind that the rate equations for the C_6 fraction were obtained with a molar H_2S to H_2 ratio of approximately 10^{-4}, i.e., 10 times higher than in the present work. Beltramini et al. (1983) and Parera et al. (1984) did not observe any significant difference between C_6 and C_7 hydrocarbons. Possibly coke deposition was decreased during the study of the C_6 fraction by Marin and Froment (1982) because of the higher H_2S to H_2 ratio. Barbier et al. (1984b) observed coke contents 4 times lower on Al_2O_3–Cl than on the corresponding Pt/Al_2O_3–Cl catalyst and suggested that platinum catalyzes coke formation by converting polycyclopentadiene species into polyaromatics. An increase of the H_2S/H_2 ratio may hamper this conversion.

Conclusions

An adequate set of Hougen–Watson rate equations has been developed for the reforming of C_7 hydrocarbons on a sulfided commercial Pt/Al_2O_3 catalyst. The selected rate equations correspond to a rate-determining step on the acid function involving a single active site. A comparison with data obtained from experiments with a C_6 fraction shows that the bifunctional reforming reaction rates increase with increasing carbon number, in agreement with carbenium ion chemistry.

The kinetics of the reforming reactions under deactivating conditions can be described by multiplying the reaction rates with a deactivation function exponentially decreasing with the coke content of the catalyst. The decreases of the rates of the bifunctional reforming reactions and of the dehydrogenation of methylcyclohexane into toluene closely agree. The deactivation constant for the coking itself is almost twice that for the reforming reactions. Coke deposition mainly originates from intercondensation between diolefinic naphthenes and toluene.

Acknowledgment

P.A.V.T. is grateful to IWONL–IRSIA for a fellowship over the years 1981–1984. The Belgian Ministry of Scientific Affairs is acknowledged for a "Center of Excellence" grant awarded within the framework of the "Concerted Actions on Catalysis".

Nomenclature

A_0, $A_{0,C}$ = preexponential factors for gas-phase reactions and coking reactions, kmol/(kg of catalyst h bar^n)

Bz = benzene
C = coke
C_C = coke content, kg of coke/kg of catalyst
C_P = coke precursor
C_5^-, C_6^- = lumps of cracked products with less than six or seven carbon atoms
DMB = lumped dimethylbutanes
2,2-DMB = 2,2-dimethylbutane
2,3-DMB = 2,3-dimethylbutane
DMCP = lumped dimethylcyclopentanes
E = apparent activation energy, kJ/mol
ECP = ethylcyclopentane
F_j = molar flow rate of jth component, kmol/h
F_{HC} = hydrocarbon molar flow rate, kmol/h
H = hydrogen or molar enthalpy, kJ/mol
k = reaction rate coefficient, kmol/(kg of catalyst h bar^n) or kg of coke/(kg of catalyst h bar^n)
K = equilibrium constant, adsorption coefficient
MCP = methylcyclopentane
$MCP^{2=}$ = methylcyclopentadiene
MCH = methylcyclohexane
$MCH^{2=}$ = methylcyclohexadiene
MBP_7 = multibranched isoheptanes
$MP^{2=}$ = methylpentadienes
2MP = 2-methylpentane
3MP = 3-methylpentane
2MH = 2-methylhexane
3MH = 3-methylhexane
P_7 = paraffins with seven carbon atoms
nP_6 = n-hexane
nP_7 = n-heptane
$nP^=_7$ = n-heptenes
N_7 = naphthenes with seven carbon atoms
$5N_7$ = five-ring naphthenes with seven carbon atoms
$5N^{2=}_7$ = cyclopentadienes with seven carbon atoms
$6N_7$ = six-ring naphthenes with seven carbon atoms
p_j = partial pressure of jth component, bar
$p(z_i,t_j)$ = matrix with the partial pressures of the independent components
r, r_i = reaction rate, kmol/(kg of catalyst h)
r_{Ck} = rate of coke formation of coking reaction k, kg of coke/(kg of catalyst h)
R = ideal gas constant, kg/(mol K)
R_j = production rate of component j, kmol/(kg of catalyst h)
R_C = coke production rate, kg of coke/(kg of catalyst h)
$\mathbf{R}$ = vector of production rates of the independent components
s_{ij} = stoichiometric coefficient of component j in reaction i
SBP_6 = single-branched isohexanes
SBP_7 = single-branched isoheptanes
t, t_j = process time, h
t_f = process time at end of deactivation run, h
T = temperature, K
Tol = toluene
W = catalyst mass, kg
x_j = fractional conversion of component j
$\mathbf{x}$ = vector of independent fractional conversions
z = axial reactor coordinate, $z = W/\rho_B\Omega$, m_r

Greek Symbols

α = deactivation constant, kg of catalyst/kg of coke
Γ = adsorption term for the acid function in Hougen–Watson rate equations
θ = adsorption term for the metal function in Hougen–Watson rate equations
ρ_B = bulk density of the catalyst bed, kg of catalyst/m_r^3
ϕ = deactivation function
Ω = cross section of reactor, m_r^3

Subscripts

A, B = with respect to component A, B
A = acid
A → B = reaction from A to B
C = coke, coking reaction
m = mean
M = metal
t = total

Superscripts

° = in absence of coke, inlet condition
^ = calculated

Registry No. Heptane, 142-82-5.

Literature Cited

Bakulin, R. A.; Levinter, M. E.; Unger, F. G. *Int. Chem. Eng.* **1978**, *18*, 89.

Barbier, J.; Elassal, L.; Gnep, N. S.; Guisnet, M.; Molina, W.; Zhang, Y. R.; Bournonville, J. P.; Franck, J. P. *Bull. Soc. Chim. Fr.* **1984a**, I-245; **1984b**, I-249.

Beltramini, J. N.; Martinelli, E. E.; Churin, E. J.; Figoli, N. S.; Parera, J. M. *Appl. Catal.* **1983**, *7*, 43.

Brandenberger, S. G.; Callender, W. G.; Meerbott, W. K. *J. Catal.* **1976**, *42*, 282.

Callender, W. L.; Brandenberger, S. G.; Meerbott, W. K. *Catal. Proc. Int. Congr., 5th, 1972* **1973**, 1265.

De Pauw, R. P.; Froment, G. F. *Chem. Eng. Sci.* **1975**, *30*, 789–801.

Froment, G. F. *Proc. Int. Congr. Catal. 6th, 1976* **1977**, *1*, 10.

Froment, G. F.; Bischoff, K. B. *Chem. Eng. Sci.* **1961**, *16*, 189.

Froment, G. F.; Bischoff, K. B. *Chem. Eng. Sci.* **1962**, *17*, 105.

Froment, G. F.; Hosten, L. H. *Catalysis Science and Technology*; Anderson, J. R., Boudart, M., Eds.; Springer-Verlag: Berlin, 1981; Vol. 2, p 97.

Heinemann, H.; Mills, G. A.; Shalit, H.; Briggs, W. S. *Brennst. Chem.* **1954**, *35*, 368.

Hosten, L. H.; Froment, G. F. *Ind. Eng. Chem. Process Des. Dev.* **1971**, *10*, 280.

Kuo, J. C.; Wei, J. *Ind. Eng. Chem. Fundam.* **1969**, *8*, 124.

Lambrecht, G.; Froment, G. F. *Proceedings of the 2nd International Symposium on Chemical Reaction*; Elsevier: Amsterdam, 1972.

Marin, G. B. Ph.D. Dissertation, University of Gent, 1980.

Marin, G. B.; Froment, G. F. *Chem. Eng. Sci.* **1982**, *37*, 759.

Menon, P. G.; Marin, G. B.; Froment, G. F. *Ind. Eng. Chem. Process Des. Dev.* **1982**, *21*, 52.

Parera, J. M.; Figoli, N. S.; Beltramini, J. N.; Churin, E. J.; Cabrol, R. A. *Proceedings of the 8th International Congress on Catalysis, 1984*; Verlag Chemie: Berlin, 1984; Vol. 2, p 593.

Van Trimpont, P. A.; Marin, G. B.; Froment, G. F. *Appl. Catal.* **1985**, *17*, 161.

Van Trimpont, P. A.; Marin, G. B.; Froment, G. F. *Ind. Eng. Chem. Fundam.* **1986**, *25*, 544.

Received for review September 23, 1985
Accepted February 24, 1986